SPREAD OF COVID-19 THROUGH N-STEP PERCOLATING PROCESS

Arpita Ganguly[1]
Scottish Church College, Department of Physics, Kolkata 700006, India

Suchetana Chatterjee[1]
Scottish Church College, Department of Physics, Kolkata 700006, India

Dr. Upendranath Nandi[2]
Assistant Professor, Scottish Church College, Department of Physics, Kolkata 700006, India

The spreading of the SARS-CoV2 virus has similar dynamics and trends to that of cluster formation and percolation in chaotic and non-linear systems. In any population, the virus begins as a small perturbation, spreads through the system exponentially and eventually saturates. This is remarkably similar to that of percolation models of any chaotic system or turbulent flow. Growth of number of infected people N_p by SARS-CoV2 virus is modeled as N-step hops through various channels formed in different populations across the world, utilising the N-channel multi-step model proposed by Glazmann-Matveev, and explaining it in terms of the principles of percolation. It is seen that the growth of N_p in various countries is well replicated by this model and can be used for accurate predictions. The transmission of the virus in Phase-I, Phase-II and Phase-III of the COVID wave is well described by this model. However, prediction after saturation point and subsequent decrease in N_p is beyond the scope of this model. Studies in this paper have been done on population densities of different countries and Indian states.

1 INTRODUCTION

Percolation theory aims to describe the behavior of chaotic systems and phase transitions, examining how different systems behave near critical points of phase change. It demonstrates how small, isolated clustered components in a system can come together and spread throughout the material through formation of "nodes" or "links" and give rise to densely interconnected, complete spanning structures. In spite of its very simple rules, percolation theory has successfully been applied to describe a large number of natural, technological and social systems with its wide applications in statistical mechanics.

Percolation theory first arose in solid-state physics, but in recent years it has found more and more use in the domain of natural sciences (physics, chemistry of polymers, biology, biochemistry, and physical virology).

Let us consider a two-dimensional square lattice (6 x 6 in this case). Now, we start occupying the square cells of the lattice in a random manner. We assume N to be the total number of cells and n to be the number of cells occupied at any instant. We define p as the fraction of occupation as $p = n/N$. There exists a critical threshold p_c, and for all values of p lesser than p_c, small randomized clusters begin to appear in the lattice but the two opposite sides of the lattice remain disconnected. The numerical value of p_c is determined by the local structure of the lattice, whereas the behavior near the critical threshold, p_c, is characterized by the behaviour of physical quantities near continuous phase transitions.

When the number of randomly occupied sites is increased, the occupation probability p rises, as does the size of each particular cluster. Upon continuing this process we eventually reach and surpass the critical threshold p_c, after which we see a spanning cluster emerge that connects the two ends of the lattice system. This uninterrupted cluster is referred to as an infinite cluster. The percolation threshold, p_c, is the occupation probability p at which an infinite cluster appears for the first time in an infinite lattice. Those clusters which do not contribute to the continuous spanning path are referred to as dangling clusters or finite clusters.

Special attention is paid to the probabilities p both below and above the percolation threshold; a percolation model for which $p < p_c$ is called a sub-critical percolation model while one satisfying $p > p_c$ is called a super-critical percolation model. Because of this distinction, the value p_c is also sometimes called the phase transition point of the model as it marks the exact point of transition between the sub-critical phase $p < p_c$ and the super-critical phase $p > p_c$. Sub-critical percolation models are necessarily devoid of infinitely connected components, whereas super-critical models always contain at least one such component.

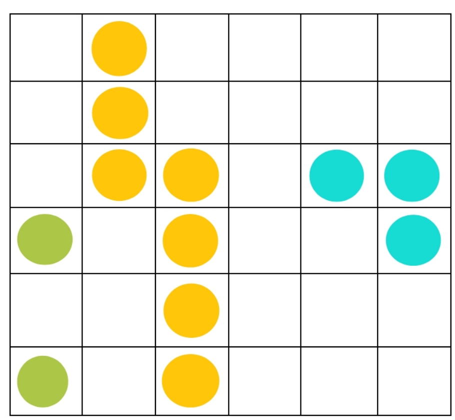

FIGURE 1. 2-D Square Lattice of dimension 6×6

In our paper, we will make use of the insight that chaotic systems eventually saturate to a definite value when left undisturbed, much like super-critical percolative systems always contain at least one infinite cluster (indicating peak saturation). Using this analogy, we correlate this to the "waves" of COVID seen in countries where the virus spreads from a small group of infected people, grows near-exponentially until it reaches a saturation limit (determined by the population's strength), and then the wave gradually recedes. We have attempted a predictive modelling of the virus for different countries and Indian states, taking this behaviour into account. The percolation problem is classically interpreted in two ways, **site percolation** and **bond percolation**. Both of these problems fall under the theory of discrete percolation. In this theory, discrete sets are taken into consideration: where, the discrete sets are lattice vertices and lattice edges.

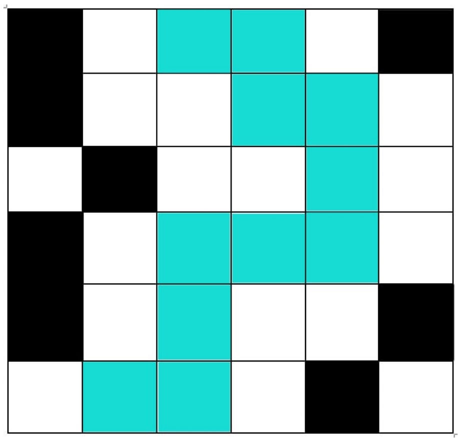

FIGURE 2. (a): Site Percolation

In site percolation, a lattice site is occupied with probability "p" or left empty in which case the probability is "$1 - p$". In site percolation, lattice vertices are considered as the relevant entities. We may refer to Fig.1 to understand this better, where the squares are occupied randomly, indicating the "sites". Two nearest-neighbor sites are connected if they are both occupied, and above the site percolation threshold, a simple spanning cluster is found to cover the entire lattice network.

In bond percolation, the lattice edges are considered as participating entities. Each edge of the lattice is open with probability p or closed with probability "$1 - p$". Two sites are said to be connected if there exists a path between them consisting of occupied bonds. The occupied bonds may represent the conducting elements of a composite material, or the high-permeability regions. The vacant bonds represent the low permeability, or impermeable regions of the pore space that contribute very little to flow or transport.

For example, the spread of SARS-CoV2 virus in any population is a classic "bond percolation" problem wherein the virus spreads from one infected person to a non-infected individual when they approach each other within the feasible distance of viral transmission. This way, a small "perturbation" (infected individual) can spread the virus to an entire population. Thus social distancing, wearing masks in public and following lockdown guidelines is important in order to break the "chain" of COVID-19 infection.

1.1 Brief Overview on Electrical Percolation

Let us begin with an introduction to the concept of percolative systems which can be successfully applied to explain the phenomenon of electrical percolation. Percolative systems are a special class of disordered materials comprising mainly of composites. A composite system is made up of conductors of a certain volume fraction (say, p) and insulators of volume fraction $(1 - p)$.

For low values of p the composite displays insulating behaviour and as the value of p is increased, the material starts showing conductive behaviour.

This change in the behaviour of the composite takes places at the percolation threshold p_c.

At p_c we notice the formation of an infinite cluster in the medium. When p approaches p_c from above, the infinite cluster is seen to be a sparse network in the gaps of which several finite and dangling clusters are located. The probability that a given bond will link a finite or an infinite number of bonds depends directly on the value of p but it is independent of the random placement of blocked and unblocked bonds .This is the percolation probability which is denoted by $P^b(p)$ where the superscript is used to indicate bond percolation. We can see $P^b(p)$ is equal to zero for lower values of p and $P^b(p) \rightarrow 1$ as $p \rightarrow 1$.[1]

Many percolative systems like composites, nanostructures etc are complex in nature, with the presence of an inherent disorder in them. Such disordered systems form a unique class of materials having localized states in common and are ideal for the investigation of electric, magnetic and optical properties. The electrical transport properties of disordered systems include the measurement of conductivity both in linear and nonlinear regions.

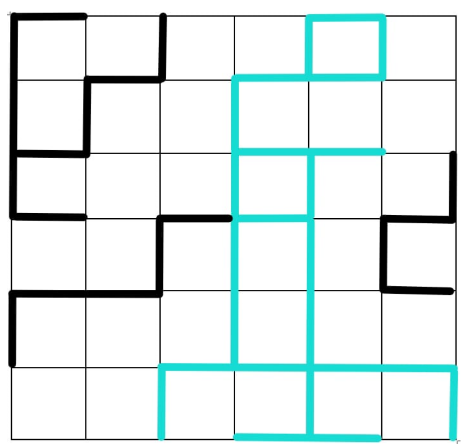

FIGURE 3. (a): Bond Percolation

In this paper, the model that we have worked with is inspired fully by the Glazmann-Matveev model which is established on the basics of electrical percolation. The Glazmann-Matveev Model attempts to describe conduction mechanisms in disordered, percolative systems. In case of electronic transport through a thin amorphous layer (thickness less than the localization length), conduction takes place in form of the direct tunneling process. With an increase in the barrier thickness, it is noticed that the conductance depends on the temperature and the bias voltage as a power law. In such a situation, both elastic and inelastic "hopping" of electrons occur through the metal–insulator junction. Glazmann and Matveev (GM) proposed a microscopic model to study the process of inelastic tunneling through two localized states. Electric field activated nonlinear electron transport in composites is described by GM model over several separate channels of conduction.

1.2 Percolation and the Spread of Corona Virus

In this section, we are aiming to propose an appropriate predictive model for the growth and spread of SARS-CoV2 virus all over the globe, in different populations. The model is based on the spreading of the virus via n-step "hopping" through various channels. Such channels may extend beyond the border of a specific country, or state, and cause a global threat. This is, on principle, similar to the n-channel multi-step model proposed by Glazmann-Matveev, in which the electrical conduction in a disordered system is derived via n-step inelastic tunneling of electrons through various channels formed by the localized states. It is intriguing to observe the growth propagation of the novel coronavirus in any population by observing its similarities to electron tunneling.

We believe it is worthwhile to pursue and look into this analogy between the two phenomena as they are closely connected to each other at their very fundamentals. Both of them can be explained through the principle of percolation. Even though they are taking place in wildly different mediums, they follow the same concepts of propagation : in the case of the GM Model, it is prominently a case of an electric percolative system, whereas the spread of the novel coronavirus in a population resembles simply a chaotic system reaching saturation through the formation of "bonding connections" between different individuals in the "lattice" of the population. Here, we will attempt to perform predictive work by looking into the curiously similar behaviors of these two systems.

The fact that every chaotic system saturates to a finite value, even though this value might be very large, indicates that the "phase-space" of the system is limited and reflects some conservation laws, such as energy conservation for a physical system. This observation is analogous to the behavior of microscopic systems that have been sufficiently explained through the principles of percolation previously. The SARS-CoV2 virus spreads directly, from infected person to non-infected person, through air droplets generated by sneezing, coughing, or close personal contact with said person, over a distance of approximately six meters. Thus we can see, contact or "bond" is established between an infected person and their nearest neighbors whenever they come into the range viable for infecting each other. In this way, we can visualize the virus spreading through a population through different "channels" not unlike the way a small perturbation might develop and percolate through a chaotic system, stopping only when it reaches the "saturation region" for that system; or, in this case, the maximum number of infected people in a certain population.

Even though several vaccines have been created to fight against the SARS-CoV2 virus, they only serve as a preventive measure that does not allow the severity of the disease to escalate; they do not guarantee that a vaccinated person will never be infected with the virus. With the absence of a guaranteed cure for the ever-mutating virus, only preventive measures can be taken; maintaining social distancing in public spaces, disinfecting hands with hand sanitizer, practicing proper coughing etiquette, wearing masks and obeying lockdown regulations.

As we have seen in the percolation model, the virus is the most dangerous if the probability of transmission (or the bond probability p in the percolation model) is high. Thus, we can arrive at a relation with the population density, ρ_s, which must be higher than a certain value to enable substantial infectious spread (say, $\rho_s > 1000$ persons per km^2).
A perturbation in such a population grows with more vigour and affects nearby places which are a distance x from it. Therefore , this spreading is governed by the ratio, $\rho = \rho_s/x$
Even though state and national governments throughout the world were quick in introducing "Lockdown"s to help break the infection chain as a hard protective measure, a lot of responsibility falls on individuals and their cooperation to make these measures successful. "Patient zero" is described as the first confirmed case in a population, from which a bulk of the final cases eventually originate. In a lot of indian states, the patient zero was a person traveling from other states while violating covid restrictions, refusing to self isolate and mixing freely with the population. Thus it is the responsibility of an individual to be mindful of following the lockdown guidelines.

2 Analysis

Figure 4 and Figure 5 show the variation of number of infected people (N_P) by the SARS-CoV2 virus as a function of number of days (N_D) in ten Indian States and eleven selected countries respectively. We aim to study the efficiency of our model by increasing and diversifying the sample test space (By considering populations of countries as well as considering populations of Indian States). The most interesting aspect is clearly seeing how every single population follows the same trend in respect to infectious spread. In both cases, the characteristic features of the variables are as follows: N_P is initially very small as expected, indicating the existence of Phase-I shown against the curve corresponding to Maharashtra (Figure 5) and China (Figure 4). With the increase in N_D, N_P starts deviating from its almost constant (linear) value with an upward trend. This corresponds to onset (in terms of days, N_D^{ON}) of the associated spreading of the SARS-CoV2 and is termed as Phase-II. Basically N_D^{ON} marks the transition from Phase-I to Phase-II and is indicated in both the curves. Beyond this onset day N_D^{ON}, N_P increases almost vertically within a minimal span of N_D. This region

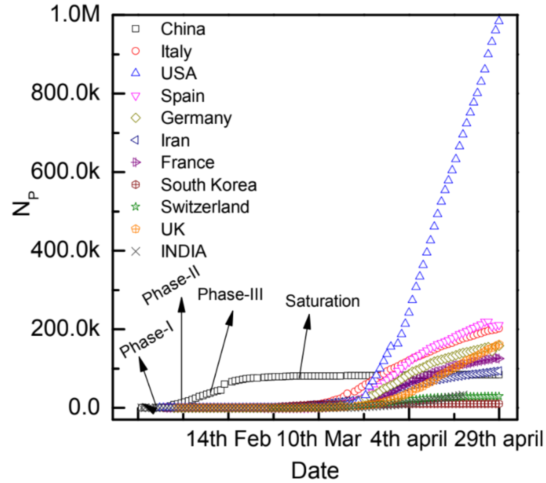

FIGURE 4. Variation of number of infected people N_P by the SARS-CoV2 virus as a function of days with date in various countries mentioned inside the graph. Only eleven countries are considered as case study. Labels have been added in the graph to distinguish between the three phases and also to indicate the saturation phase. Data plotted is taken from the very onset of the COVID-19 pandemic to the peak of the first wave in most countries.

of the sharp increase in N_P is termed as Phase-III. In this stage, the SARS-CoV2 virus almost forms a connected "infinite cluster" of N_P through the infected population, leading to disruption of normal activities. If the virus is left to spread unrestrained in Phase-III, the consequences could be devastating. This is the ideal time for implementation of hard preventive measures : full lockdowns, night curfews, etc. Finally, with all sorts of these comprehensive measures taken, the rate of increase in N_P decreases with further increase in N_D, and N_P approaches saturation. A notable feature of figure 4 and 5 is that Phase-I continues for more extended period in some countries and states, indicating the presence of strong measures taken up by the respective Governments against the spreading of the SARS-CoV2 virus. In the regions where the government has slacked off on the preventive measures prematurely, it has seen fast and rapid transition into the next Phase of the pandemic. For the Indian states, the trend of infection is almost the same for all the states considered, the only difference being the number of people that are affected. This is because the population density varies greatly from state to state and it is also a measure of how effective are the measures taken by the respective state governments.
Note to keep in mind while we analyze the predictive fitted data : we are seeing what the final results would look like if the virus was left to spread unrestrained through the population. Comparing these against the government data for SARS-CoV2, we can comment on the efficacy of steps taken by each state government in response to the outbreak. In some states, the final saturation value is lower than the predicted one, which points to the effectiveness of the preventive measures taken by the government.

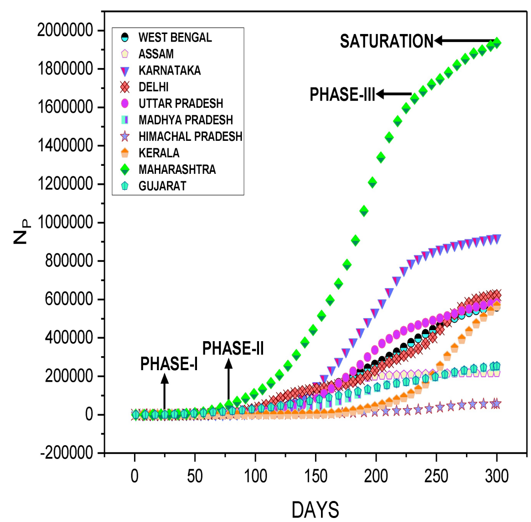

FIGURE 5. Variation of number of infected people N_P by the SARS-CoV2 virus as a function of days in various Indian States mentioned inside the graph. Ten states are are considered in this plot.

In some states, the predictive curve almost coincides with the collected data, indicating a massive surge in infections which could only have been enabled by the completely unrestrained spread of the virus across the population. Since we are not using any variable that represents the preventive measures taken in a population, this model can be useful to apply in Phase-I or Phase-II of any COVID-19 wave to see what the predicted numbers will be like at the saturation point, and attempt to take steps to reduce that projected number.
Making use of the similar dynamics of spread in each state and country, we have fitted the government data in each case to our model. As we see in Figure 7, the fit from our model replicates the data very well and can be used to make accurate predictions just up until the saturation point. After the saturation point is reached, further prediction is beyond the scope of this model. We believe this is a more accurate fit of the collected data than using a power law exponential model.

3 Model

The model we have applied to explain the spread of the virus is elaborated below. Suppose the SARS-CoV2 infects a person at location "X" at a certain instant of time t. Another person at location "Y" may be infected by "X" at an another instant of time $(t+\Delta t)$ through the following processes: (i) direct contact with "X"; (ii) indirect contact via $X \to P \to Y$; (iii) indirect contact via $X \to P \to Q \to Y$; (iv) indirect contact via $X \to P \to Q \to R \to Y$ etc. Here P, Q and R are infected persons in successive steps. Such processes are similar to direct hopping, indirect hopping through one localized state, indirect hopping through two localized states, and indirect hopping through three localized states of electrons in disordered systems in the Glazmann-Matveev (GM) model [2]. In this GM model, under an electrical bias V ($eV \gg K_BT$, e is the charge of the electron)K_B is the Boltzmann constant and T is the temperature at absolute scale), the electrical current in a disordered system is governed by the n-step tunneling of electrons through various channels. This model has been applied to explain the non-Ohmic electrical conduction in conducting polymers [3], simple and double perovskite compounds [4], and strongly correlated systems [5].

The number of infected people N_P by the SARS-CoV2 virus is a function of the number of days N_D and also depends on quantities like awareness, social contacts, and population density, etc. Following the analogy of electrical current in a disordered system as calculated in the GM model [2], N_P can be expressed as

$$\begin{aligned} N_P \quad = \quad & A_0 + A_1 N_D^1 + A_2 N_D^{2.33} + A_3 N_D^{3.5} + A_4 N_D^{4.6} + \\ & A_5 N_D^{5.67} + A_6 N_D^{6.71} + ... + A_n N_D^{p_n} + ... \qquad (1) \end{aligned}$$

where A_n are the coefficients of different channels through which the SARS-CoV2 virus spreads and $p_n = 1 + \frac{n^2+n-2}{n+1}$ with $n \geq 1$.

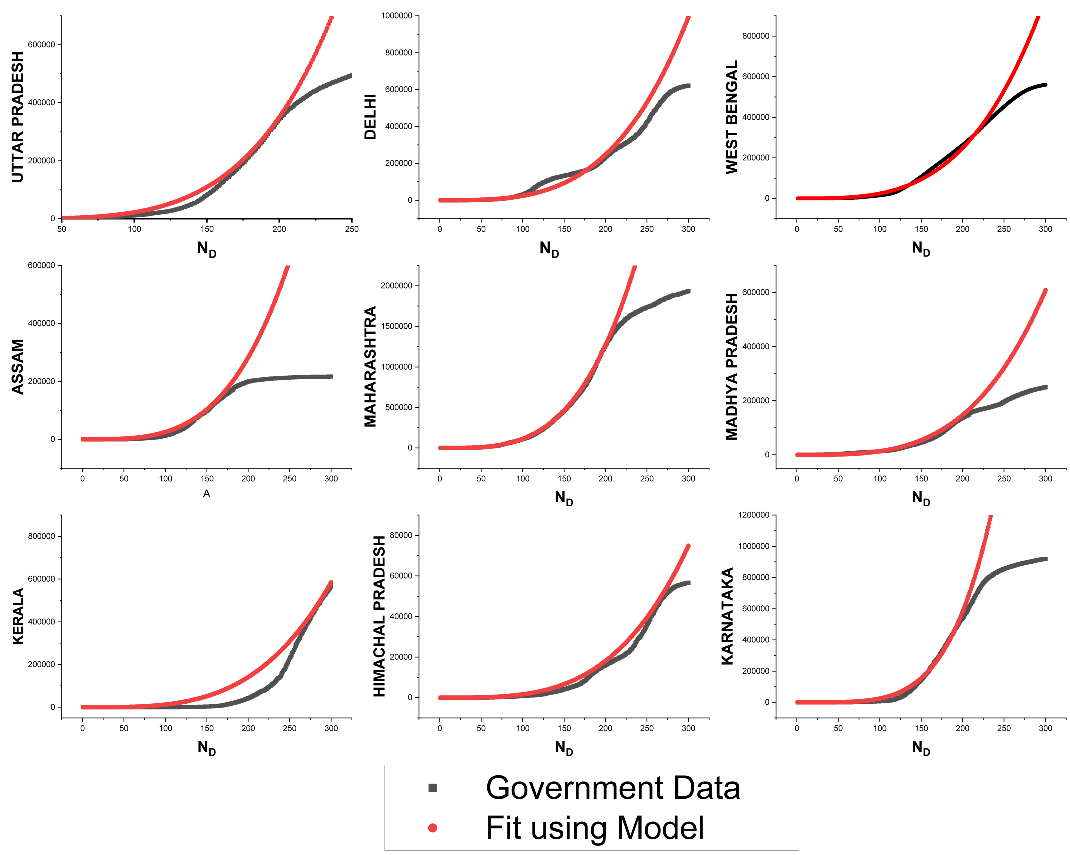

FIGURE 6. Number of people infected daily plotted as a function of number of days, for nine Indian States. Our model according to Equation is fitted alongside data provided by the government. Comparing these graphs (plotted over the same time period) gives us an insight into the efficacy of regulations implemented in each state. We can comment on the good handling of the situation in Assam because of the greater amount of time it took for the COVID-19 wave to transition from Phase - I to Phase - II. In Delhi, we see a concerning rise in cases that manages to override even the predicted value. This is also evident by seeing how badly Delhi was affected when compared to the other states.

A_0 represents the contribution to N_P due to direct contact (process (i)); A_1 represents the contribution to N_P due to indirect contact via one infected person (process (ii)) etc. N_P increases nonlinearly with N_D due to the appearance of additional channels and the multiplicity of such channels. N_P increases almost vertically beyond N_D^{ON} in Phase-III. Such a characteristic feature is observed in virtually all countries as well as states surveyed (see figures 4 and 5). The solid lines in Figure 6 are fits to N_P vs N_D data with Eq. (1) leading up to just before saturation. Data for Italy, for example, was best fitted with $A_0 = 220$, $A_1 = 80$, $A_2 = 9$, and $A_3 = 2.5 \times 10^{-1}$. Data for Himachal Pradesh was best fitted with $A_0 = 2$, $A_1 = 0.001$, $A_2 = 8 \times 10^{-4}$, and $A_3 = 0.00016$. Fits for other states and countries were also found to be excellent which implies that Eq. (1) is a valid description of the growth of the SARS-CoV2 infected people.

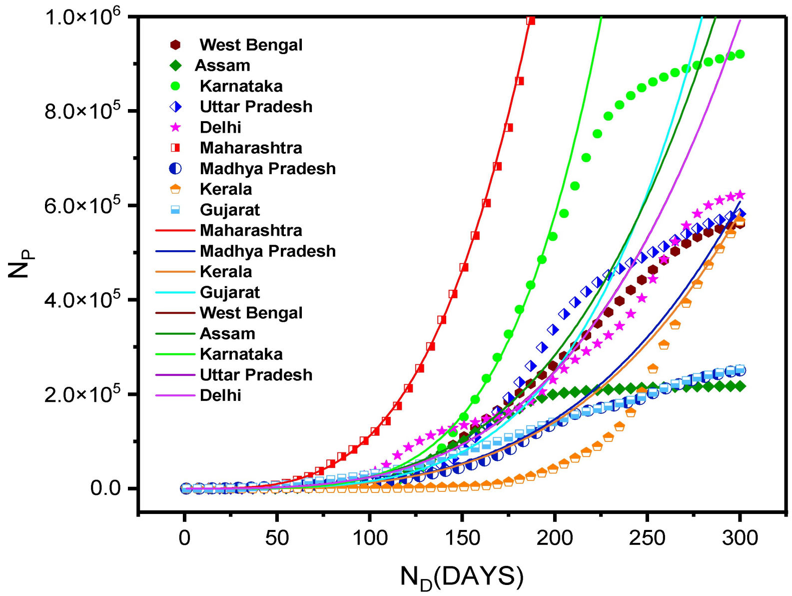

FIGURE 7. Best fit of our model against collected data for nine Indian states.

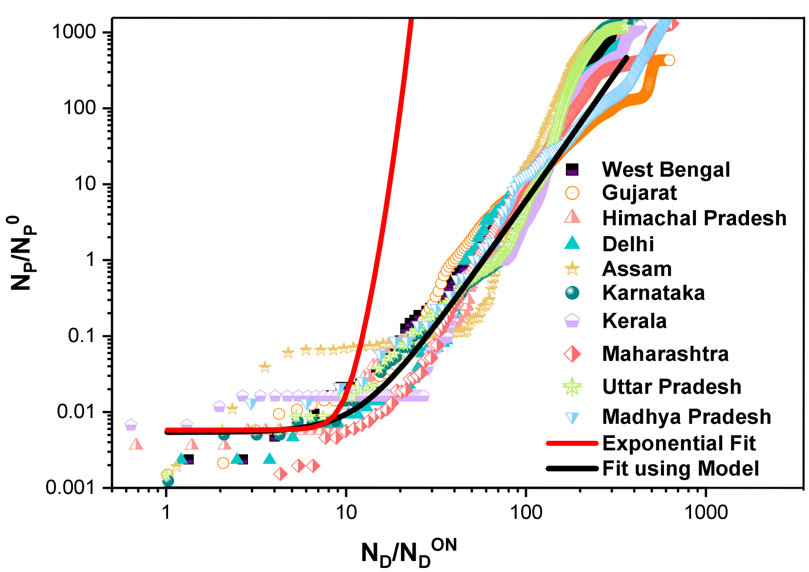

FIGURE 8. Shows the variation of $\frac{N_P}{N_P^0}$ vs. $\frac{N_D}{N_D^{ON}}$ data using the data collapse method. The black solid line is a fit according to Eq. (3). The red solid line is a fit to the scaled data according to Eq. (4). Inset shows a log-log plot of the onset day N_D^{ON} with the population N_0 of the surveyed Indian states.

Similarity in the variation of $N_P - N_D$ curves for different countries shown in figures 2 indicates that these curves could be collapsed into a single master curve using the data collapse method [6, 7, 8]. The results of such data collapse into a master curve are illustrated in Figure 8 (representing the Indian States) and Figure 10 (representing the eleven countries) in which $\frac{N_P}{N_P^0}$ vs. $\frac{N_D}{N_D^{ON}}$ data are shown in a log-log plot. In this data collapse method, N_P corresponding to a particular state, say Kerala, was divided by its linear value N_P^0 and N_D was kept unaltered, i.e., the onset day N_D^{ON} corresponding to this curve was considered to be 1. For the next state, N_P was divided by its initial value N_P^0 as before but N_D was adjusted in such a way that $N_P - N_D$ curve merged with the earlier one as best as possible. This procedure was then repeated for other states, as well as the eleven countries. The remarkable data collapse before saturation is shown in figures . In order to express that Eq. (1) is a compatible scaling form, we make the following assumption

$$A_n = B_n N_P^0 \left(N_D^{ON}\right)^{-p_n} \tag{2}$$

where $n \geq 1$, $B_n's$ are positive constants, independent of N_P^0 and $B_0 = \frac{A_0}{N_P^0}$. This assumption is further supported by the experimental observation i.e. A_n decreases with the increase in N_D^{ON}. Using Eq. (2), Eq. (1) can be expressed in the following scaled form

$$\begin{aligned}\frac{N_P}{N_P^0} &= B_0 + B_1 x^1 + B_2 x^{2.33} + B_3 x^{3.5} + B_4 x^{4.6} + \\ &\quad B_5 x^{5.67} + B_6 x^{6.71} + ... + B_n x^{p_n} + ...\end{aligned} \tag{3}$$

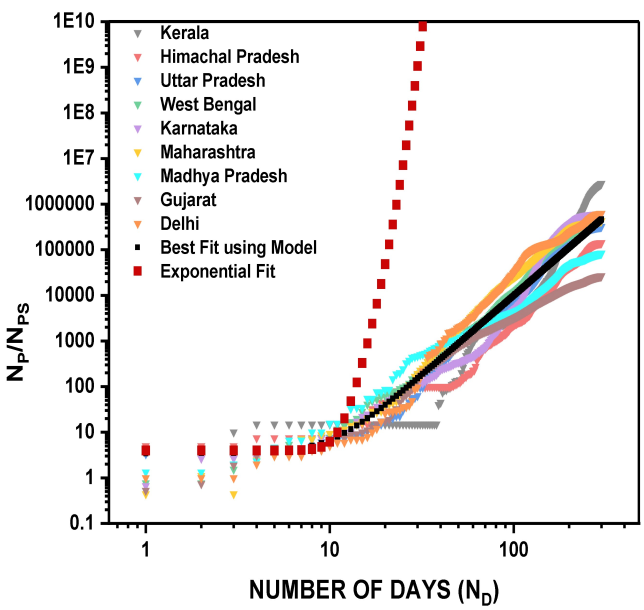

FIGURE 9. A scaled representation of COVID-19 data for the nine Indian states, showing fit using our model and exponential fit.

Here N_P^0 is the number of people infected initially, and $x = \frac{N_D}{N_D^{ON}}$. The solid line (blacken bold) in figure 8 is a fit to the scaled data, according to Eq. (3) with the following values of the coefficients:
$B_0 = 0.0055$, $B_1 = 1 \times 10^{-5}$, $B_2 = 9 \times 10^{-6}$, and $B_3 = 1 \times 10^{-6}$. Such fit is really impressive, signifying the common characteristics of the data.

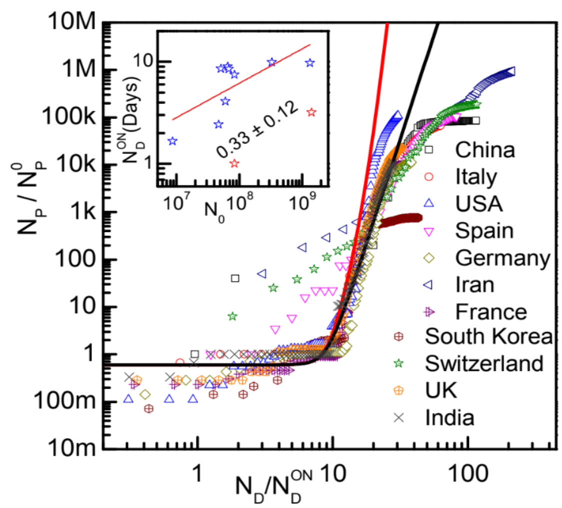

FIGURE 10. Shows the variation of $\frac{N_P}{N_P^0}$ vs. $\frac{N_D}{N_D^{ON}}$ data following the data collapse method. The black solid line is a fit according to Eq. (3). The red solid is a fit to the scaled data according to Eq. (4). Inset shows a log-log plot of the onset day N_D^{ON} with the population N_0 of the surveyed countries. See text for details.

$$\frac{N_P}{N_P^0} = 0.0055 + G_0 e^x \tag{4}$$

The red solid line in figure 8 is a fit according to the equation with $G_0 = 1 \times 10^{-6}$. Though the fit with Eq. (4) is reasonably good in Phase-II but its deviation from the scaled data in Phase-III indicates that an exponential function given by Eq. (4) is not appropriate for the description of growth of N_P by the SARS-CoV2 virus.

Thus the model of n-step hopping through multi-channels is the most suitable one to describe the growth of N_P. To find correlation between the onset day N_D^{ON} and the population N_0 of a country, N_D^{ON} was plotted against N_0 in a log-log curve at the inset of figure 10.

4 Conclusion

In conclusion, the growth of infected people by the SARS-CoV2 virus may be predicted by a model consisting of n-step hops through multi-channels given by Eq. (3). This growth is not governed by an exponential function given by Eq. (4). We can see from Figure 6, the spread of the virus in some states has not deviated much from the projected value. Meanwhile, in some states like Kerala it has dipped below the projected value and in some like Delhi, it has risen above the modeled values. In the case of Kerala, it shows an effective handling of the pandemic which led to a controlled and slowed spread of the virus because of stringent social distancing and lockdowns. We must keep in mind, while dealing with a pandemic spread, that in a wave of infection, we cannot stop or eradicate the virus completely once it has started spreading, and nor is it a realistic goal. But while we cannot stop it from reaching its saturation point of infections, we can implement protective measures that will bring that final number down. This way, by only looking at the graphs of the individual states, we can comment on the public handling of the pandemic, and remark whether their response is efficient or not.

Though the model can accurately predict the dynamics of the spread of the SARS-CoV2 virus up until the saturation point, it cannot predict the recovery characteristic from the virus as that aspect is beyond the scope of the model.

We believe implications from our fitting and analyzing attempts go further than only applications of epidemiological predictive modeling. As we know, the growth and spread of COVID-19 in a controlled population is the case of evolution of a complex system. In our paper, we have observed similarities in the spread of the coronavirus to that of the dynamics of current spread and saturation in a conductor. These two systems, while being wildly different from each other in the respect of their constituents and properties governing them, surprisingly show similar behavior in the dynamics of their evolution and growth (albeit differing in the magnitudes of the values of their coefficients in the GM-Model equation). This leads us to wonder if such equivalence may be drawn between other natural systems, and whether a sense of generality may be established in our treatments of all complex systems. Even though some systems may be extremely different from each other, their dynamics of evolution are still restricted by some universal laws like that of energy conservation, and evolve through some similar physical processes (for example, in our paper we have shown one such processes to be percolation).

In exploring such constant qualities of all systems, we can hope to arrive at the conclusion of the presence of an overarching symmetry and universality in the behavior of all systems of matter, no matter their physical environment or chemical composition.

References

[1] U.N.Nandi, Debnarayan Jana, and D.Talukdar. "Scaling description of non-ohmic direct current conduction in disordered systems". In: *Progress in Materials Science* 71 (June 2015), pp. 1–92. DOI: https://doi.org/10.1016/j.pmatsci.2014.12.001.

[2] L. I. Glazrnan and K. A. Matveev. "Inelastic tunneling across thin amorphous films". In: *Annalen der Physik* (1988). DOI: http://jetp.ras.ru/cgi-bin/dn/e_067_06_1276.pdf.

[3] D. Talukdar et al. "Nonlinearity exponents in lightly doped conducting polymers". In: *Phys. Rev. B* 84 (August 2011). DOI: https://doi.org/10.1103/PhysRevB.84.054205.

[4] D. Talukdar et al. "Scaling of non-Ohmic conduction in strongly correlated systems". In: *Phys. Rev. B* 86 (October 2012). DOI: https://doi.org/10.1103/PhysRevB.86.165104.

[5] K. K. Bardhan et al. "Universal scaling in disordered systems and nonuniversal exponents". In: *Phys. Rev. B* 89 (May 2014). DOI: https://doi.org/10.1103/PhysRevB.89.184201.

[6] U.N.Nandi, Animesh Kr. Dey, and D.Talukdar. "Gap states controlled transmission through 1D metal-nanotube junctions". In: *Carbon* 146 (May 2019), pp. 106–115. DOI: https://doi.org/10.1016/j.carbon.2019.01.092.

[7] Animesh Kr. Dey et al. "Nonlinearity exponent: A phase sensitive parameter in disordered systems". In: *Physica B: Physics of Condensed Matter* 582 (April 2020). DOI: https://doi.org/10.1016/j.physb.2020.412001.

[8] Animesh Kr. Dey et al. "Zener-like electrical transport in polyaniline–graphene oxide nanocomposites". In: *RSC Advances* 8 (2020). DOI: https://doi.org/10.1039/C9RA07267E.